spring-damping system, in which the body, bogie and wheelset are all rigid bodies. The secondary suspension between car-body and bogie and the primary suspension between bogie and wheelset are simulated by spring-damping system.

Five independent degrees of freedom (DOF) including lateral, vertical, roll, pitch and yaw are considered for both vehicle and structure, and 4 independent degrees of freedom are considered for wheelset. Therefore, the whole carraige includes 31 independent DOFs, as shown in Table 1. The train coordinate system adopts the right-hand coordinate system.

Table 1 Train corresponding degree of freedom.

| | lateral | vertical | roll | pitch | yaw |
|---|---|---|---|---|---|
| Car-body | $y_{\mathrm{C}}$ | $z_{\mathrm{C}}$ | $\varphi_{\mathrm{C}}^{x}$ | $\varphi_{\mathrm{C}}^{y}$ | $\varphi_{\mathrm{C}}^{z}$ |
| Front bogie | $y_{\mathrm{T1}}$ | $z_{\mathrm{T1}}$ | $\varphi_{\mathrm{T1}}^{x}$ | $\varphi_{\mathrm{T1}}^{x}$ | $\varphi_{\mathrm{T1}}^{z}$ |
| Rear bogie | $y_{\mathrm{T2}}$ | $z_{\mathrm{T2}}$ | $\varphi_{\mathrm{T2}}^{x}$ | $\varphi_{\mathrm{T2}}^{x}$ | $\varphi_{\mathrm{T2}}^{z}$ |
| First wheelset | $y_{\mathrm{W1}}$ | $z_{\mathrm{W1}}$ | $\varphi_{\mathrm{W1}}^{x}$ | - | $\varphi_{\mathrm{W1}}^{z}$ |
| Second wheelset | $y_{\mathrm{W2}}$ | $z_{\mathrm{W2}}$ | $\varphi_{\mathrm{W2}}^{x}$ | - | $\varphi_{\mathrm{W2}}^{z}$ |
| Third wheelset | $y_{\mathrm{W3}}$ | $z_{\mathrm{W3}}$ | $\varphi_{\mathrm{W3}}^{x}$ | - | $\varphi_{\mathrm{W3}}^{z}$ |
| Fourth wheelset | $y_{\mathrm{W4}}$ | $z_{\mathrm{W4}}$ | $\varphi_{\mathrm{W4}}^{x}$ | - | $\varphi_{\mathrm{W4}}^{z}$ |

### *2.2. Train displacement vector.*

Taking a single train as an example, the displacement vector of the train can be expressed as,

$$\mathbf{X}^{Vi}=[\mathbf{X}_{c}^{V_i}\ \ \mathbf{X}_{t1}^{V_i}\ \ \mathbf{X}_{t2}^{V_i}\ \ \mathbf{X}_{w1}^{V_i}\ \ \mathbf{X}_{w2}^{V_i}\ \ \mathbf{X}_{w3}^{V_i}\ \ \mathbf{X}_{v4}^{V_i}]^{\mathrm{T}} \tag{1}$$

with $\mathbf{X}_{\mathrm{c}}^{Vi}=[y_c\ \ z_c\ \ \varphi_{\mathrm{c}}^{x}\ \ \varphi_{\mathrm{c}}^{y}\ \ \varphi_{\mathrm{c}}^{z}]^{\mathrm{T}}$; $\mathbf{X}_{tj}^{Vi}=[y_{tj}\ \ z_{tj}\ \ \varphi_{tj}^{x}\ \ \varphi_{tj}^{y}\ \ \varphi_{tj}^{z}]^{\mathrm{T}}, j=1,2$;

$\mathbf{X}_{wj}^{V_i}=[y_{wj}\ \ z_{wj}\ \ \varphi_{wj}^{x}\ \ \varphi_{wj}^{z}]^{\mathrm{T}}, j=1,2,3,4$.

### *2.3. Train dynamics equation*

The principle of elastic potential energy invariability and the principle of "taking the right seat" (Zeng 1999) can quickly obtain the dynamic equation of the time-varying system of train-track-bridge. In this paper, the mass, stiffness and damping matrices of the train are obtained by this theory. The dynamic equation of the train is

$$\mathbf{M}^{V}\ddot{\mathbf{X}}^{V}+\mathbf{C}^{V}\dot{\mathbf{X}}^{V}+\mathbf{K}^{V}\mathbf{X}^{V}=\mathbf{F}^{V} \tag{2}$$

where $\mathbf{M}^{V}$, $\mathbf{C}^{V}$ and $\mathbf{K}^{V}$ are the mass, damping and stiffness matric of train, respectively; $\mathbf{X}^{V}, \dot{\mathbf{X}}^{V}$ and $\ddot{\mathbf{X}}^{V}$ are the displacement, velocity and acceleration vector of

train, respectively; The load vector $\mathbf{F}^{v}$ includes the gravity of the train itself, the force generated by seismic acceleration and the force generated by wheel rail contact. The wheel-rail force is more complex and will be described in section 2.4.

*2.4. Wheel-rail contact.*

The normal force and creep force of wheel-rail are produced by wheel rail contact. The train and track bridge structure are coupled into a large system through the wheel rail relationship. In this paper, the wheel-rail contact is assumed to be knife-edge contact constraints (Cheng 2017; Zeng 2018), that is, the ideal conical tread, and the rail is regarded as a hinge point. As shown in Fig. 2, the lateral clearance between wheel and rail is 10 mm, and the lateral contact stiffness $k_{ry}$ is $1.617\times10^{7}$N/m (Cheng 2017).

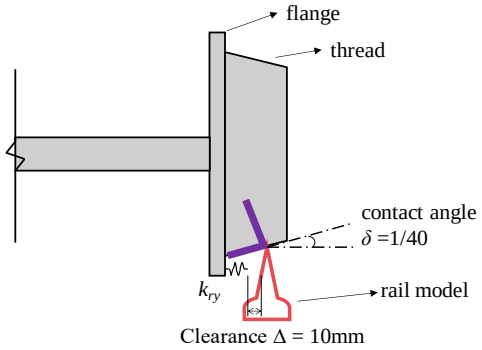


Fig. 2 Wheel-rail contact.

The wheel rail vertical force is calculated by Hertz contact theory, which can be expressed as

$$P_{hz} = G^{-1.5}\Delta_{wr}^{1.5} \tag{3}$$

where $G$ is the constant; $\Delta_{wr}$ is the wheel-rail relative compression, and according to the displacement relationship, the compression of Hertz spring can be obtained by simplified calculation,

$$\begin{cases} \Delta_{wr,i}^{L} = -\left(z_{\mathrm{W}_i} + b_w\varphi_{\mathrm{W}_i}^{x} - z_{Ri}^{L}\right), & \text{if } \Delta_{wr,i}^{L} < 0, \Delta_{wr,i}^{L} = 0 \\ \Delta_{wr,i}^{R} = -\left(z_{\mathrm{W}i} - b_w\varphi_{\mathrm{W}i}^{x} - z_{Ri}^{R}\right), & \text{if } \Delta_{wr,i}^{R} < 0, \Delta_{wr,t}^{R} = 0 \end{cases} \tag{4}$$

where the subscript $i$ represents the $i^{\text{th}}$ wheelset and the corresponding rail position; the superscript $R$ and $L$ represent the right and left rail respectively; $z_{Ri}^{L}$ and $z_{Ri}^{R}$ are the vertical displacement of the left and right rail respectively.

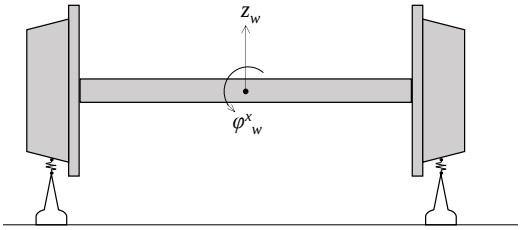


Fig. 3 Calculation of wheel-rail contact geometric state.

Kalker linear creep force model (Kalker 1967) is adopted for the creep force, and Shen–Hedrick–Euristic (Shen 1983) nonlinear creep model is used for large creep.

*2.5. Track-bridge model of HSR.*

In this paper, the finite element method (FEM) is used to establish the track-bridge system. The spatial Euler-Bernoulli beam element is used to simulate the rail, track slab, bridge and pier. The fastener between rail and track plate is connected by discrete spring damping. The bearing between the main beam and the pier is connected by spring damping. The bottom of the pier is connected with the earth by spring damping. As the main research object of this paper is bridge structure, in order to reduce the degree of freedom, the subgrade section is assumed to be rail rigid subgrade. The damping of bridge structure is relatively complex, and the comprehensive effect of structural damping can be simulated by proportional damping (Liu 2020a), which is simplified as the proportional combination of mass and stiffness

$$\mathbf{C}^b = \alpha \mathbf{M}^b + \beta \mathbf{K}^b \tag{5}$$

where $\mathbf{M}^B$ and $\mathbf{K}^B$ are mass and stiffness matrix of structures. For common Rayleigh damping, there are:

$$\begin{cases} \alpha = 2\omega_1\omega_2 \dfrac{\xi_2\omega_1 - \xi_1\omega_2}{\omega_1^2 - \omega_2^2} \\ \beta = 2\dfrac{\xi_1\omega_1 - \xi_2\omega_2}{\omega_1^2 - \omega_2^2} \end{cases} \tag{6}$$

where $\omega_1$ and $\omega_2$ are the first and second order natural frequencies of structures; $\xi_1$ and $\xi_2$ are the damping ratio of the first two modes.

The stiffness, mass and damping matrices are assembled by the FEM to obtain the overall stiffness, mass and damping matrices. Then, according to the structural dynamics, the dynamic equation of the bridge is obtained as follows

$$\mathbf{M}^B\ddot{\mathbf{X}}^B + \mathbf{C}^B\dot{\mathbf{X}}^B + \mathbf{K}^B\mathbf{X}^B = \mathbf{F}^B \tag{7}$$

where $\mathbf{X}^B$ is the displacement vector of the bridge; $\mathbf{F}^B$ is the load vector of the bridge, including the wheel rail force caused by wheel rail contact and the inertial force generated by seismic excitation.

*2.6 Dynamic equation of the system.*

By combining Eqs.(2) and (7), the dynamic equation of the system can be obtained as follows

$$\begin{cases} \mathbf{M}^V \ddot{\mathbf{X}}^V + \mathbf{C}^V \dot{\mathbf{X}}^V + \mathbf{K}^V \mathbf{X}^V = \mathbf{F}^V \\ \mathbf{M}^B \ddot{\mathbf{X}}^B + \mathbf{C}^B \dot{\mathbf{X}}^B + \mathbf{K}^B \mathbf{X}^B = \mathbf{F}^B \end{cases} \tag{8}$$

In this paper, Wilson-$\theta$ is used for iterative calculation.

## 3. INFLUENCE FACTOR.

*3.1. Influence of bridge natural vibration period on train operation.*

For the same seismic wave input, the dynamic response of bridge structure will change with the natural vibration characteristics of the bridge, and the change of rail response will directly affect the RS of train. In order to discuss the influence of different bridge structure natural vibration period on train RS, under the same speed (300km/h), by changing the bridge height to change the natural vibration period of bridge structure, a total of 10 kinds of pier height are calculated. The minimum value of the first transverse period is 0.104 s, and the maximum value is 1.582 s. Five ground motion (GM) samples (Kobe wave, Loma Prieta wave, Northridge wave, Tabas Iran wave and Trinidad wave (2019)) are input into the train-track-bridge system, and the maximum ground acceleration is 0.3g. The same set of samples generated from the track power spectral density function (PSD) of China's HSR are used. The maximum values of train derailment coefficient (Q/P) under different GM samples and different bridge transverse first period are shown in Fig. 4. It can be found that, except for Trinidad wave, the maximum value of train Q/P under other GM sample conditions will change obviously with the change of bridge period, and the overall trend is that the Q/P increases with the increase of the period. In addition, it can be found that the results obtained by different GM samples are quite discrete.

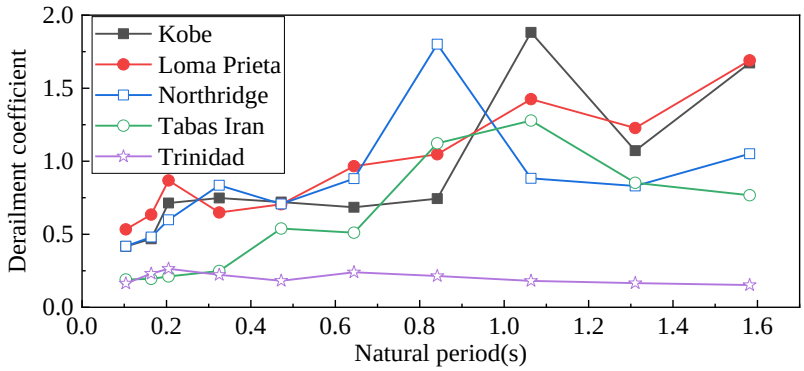


Fig. 4 Maximum value of Q/P under different structural periods.

*3.2. Influence of train speed on train running safety.*

When the train speed increases, the excitation of track irregularity is more frequent, and the creep force of wheel-rail will change with the speed, which will affect the RS of the train (Liu 2020b). The results of references (Xia 2006; Xiao 2012; Ju 2012) showed that train speed has a certain impact on the RS of HSR trains under earthquake. In order to explore the influence of vehicle speed on the RS of HSR trains on the bridge, five GM samples (consistent with section 3.1) are also selected, and the maximum ground acceleration is 0.3g. The first lateral period of the bridge is 0.3244s. The same set of samples generated from the PSD of China's HSR are used. The maximum values of Q/P corresponding to different GM samples at different speeds are obtained as shown in Fig. 5. It can be found that the maximum Q/P of the other three waves increases with the increase of vehicle speed except Tabas Iran wave and Trinidad wave.

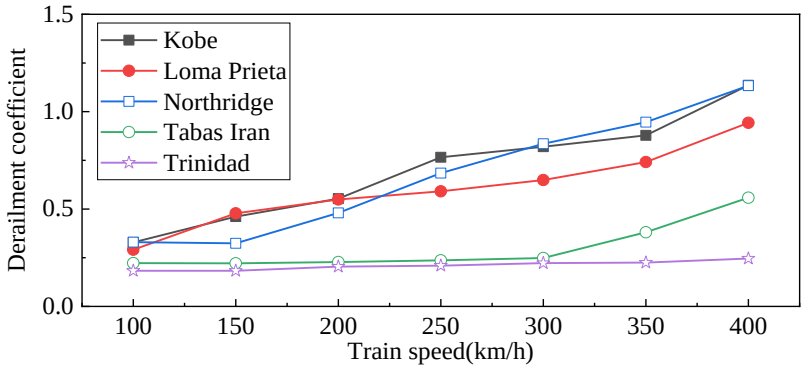


Fig. 5 Maximum value of Q/P under different train speeds.

*3.3. Influence of track irregularity on train RS.*

Track irregularity is applied to the train-track-bridge system as an incentive, which will affect the stability of the train and the RS of the train (Jiang 2019b). In order to discuss the influence of track irregularity on train RS on bridge during earthquake, two models are established, one is considering track irregularity and the other is not considering track irregularity. Three original GM samples of Kobe wave, Northridge wave and Loma Prieta wave are used. In each case, the same irregularity sample is used. The time-history curves of Q/P under two working conditions when the train running speed is 300km/h are shown in Fig. 6. It can be seen that the Q/P in the case of no track irregularity is basically unchanged, and the Q/P with track irregularity has a small amplitude oscillation before the input seismic wave. After the input of seismic waves, the Q/Ps of the two conditions change greatly, and the trend is relatively consistent. The Q/Ps of the three GM samples with irregularities are greater than those without irregularities.

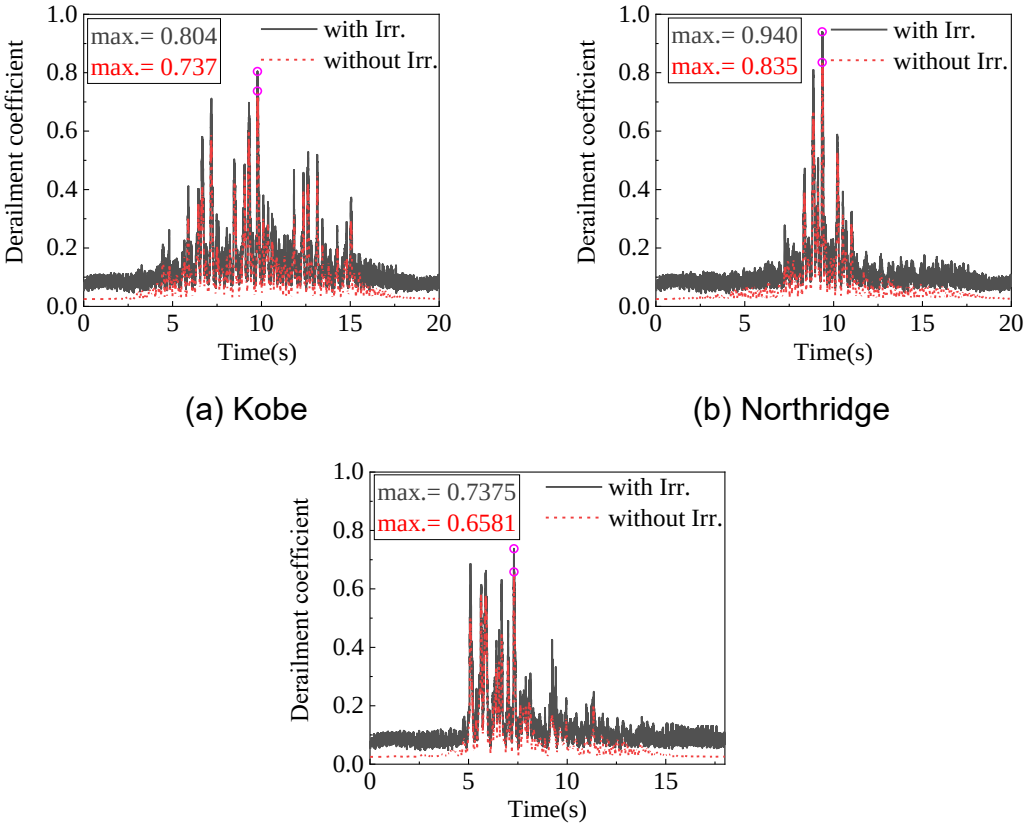


(a) Kobe

(b) Northridge

(c) Loma Prieta

Fig. 6 Time history response of Q/P with and without irregularity.

Fig. 7 shows the maximum values of Q/P under different speed conditions with and without irregularities. Generally speaking, with and without irregularities, the Q/P will increase with the increase of vehicle speed, but the increase range of different GM samples is different; in addition, the Q/P of irregularity condition is greater than that of no irregularity condition.

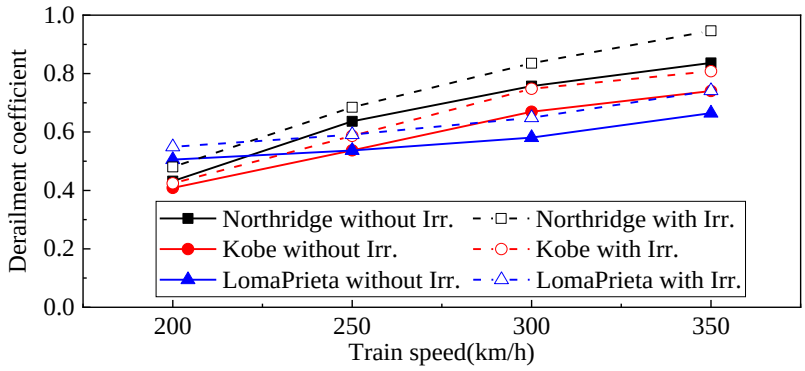


Fig. 7 The maximum values of Q/P corresponding to different speeds with and without irregularities.

## 4. CONCLUSIONS

In order to discuss the influence factor on train running safety on the bridges during earthquake, the dynamic model of train-track-bridge coupled model is established, and FEM theory is applied to simulate track-bridge system; mass-spring-dashpot systems are used to simulate the train; the knife-edge contact constraints are used to deal with wheel-rail contact. The influences of natural vibration period of bridge, train speed and track irregularity on the running safety of train are discussed. The results are as follows:

(1) The natural vibration period of the structure has a great impact on the train RS, and different ground motion samples show different results;
(2) The derailment coefficient of the train increases with the increase of the vehicle speed;
(3) The track irregularity has a certain impact on the train RS.

## ACKNOWLEDGEMENTS

The work described in this paper is supported by grants from the National Natural Science Foundation of China (Grant Nos. U1934207 and 51778630).

## REFERENCES

Cheng Y-C, Chen C-H, Hsu C-T (2017) Derailment and Dynamic Analysis of Tilting Railway Vehicles Moving Over Irregular Tracks Under Environment Forces. Int J Str Stab Dyn 17:1750098.

Du XT, Xu YL, Xia H (2012) Dynamic interaction of bridge-train system under non-uniform seismic ground motion. Earthquake Engng Struct Dyn 41:139–157.

Feng Y, Jiang L, Zhou W, et al (2019) An analytical solution to the mapping relationship between bridge structures vertical deformation and rail deformation of high-speed railway. Steel and Composite Structures 33:209–224

Jiang L, Feng Y, Zhou W, He B (2019a) Vibration characteristic analysis of high-speed railway simply supported beam bridge-track structure system. Steel and Composite Structures 31:591–600

Jiang L, Liu X, Xiang P, Zhou W (2019b) Train-bridge system dynamics analysis with uncertain parameters based on new point estimate method. Engineering Structures 199:109454.

Jin Z (2016) Effect of vertical ground motion on earthquake-induced derailment of railway vehicles over simply-supported bridges. Journal of Sound and Vibration 18

Ju SH (2012) Nonlinear analysis of high-speed trains moving on bridges during earthquakes. Nonlinear Dyn 69:173–183.

Kalker J (1967) On the rolling contact of two elastic bodies in the presence of dry friction. Delft University of Technology

Liu X, Jiang L, Lai Z, et al (2020a) Sensitivity and dynamic analysis of train-bridge coupled system with multiple random factors. Engineering Structures 221:111083.

Liu X, Xiang P, Jiang L, et al (2020b) Stochastic Analysis of Train–Bridge System Using the Karhunen–Loéve Expansion and the Point Estimate Method. Int J Str Stab Dyn.

Luo X, Miyamoto T (2007) Method for running safety assessment of railway vehicles against structural vibration displacement during earthquakes. Quarterly Report of RTRI 48:129–135

Nishimura K, Terumichi Y, Morimura T, et al (2015) Using Full Scale Experiments to Verify a Simulation Used to Analyze the Safety of Rail Vehicles During Large Earthquakes. Journal of Computational and Nonlinear Dynamics 10:031013.

Tanabe M, Matsumoto N, Wakui H, et al (2008) A Simple and Efficient Numerical Method for Dynamic Interaction Analysis of a High-Speed Train and Railway Structure During an Earthquake. Journal of Computational and Nonlinear Dynamics 3:041002.

Xia H, Han Y, Zhang N, Guo W (2006) Dynamic analysis of train–bridge system subjected to non-uniform seismic excitations. Earthquake Engng Struct Dyn 35:1563–1579.

Xiao X, Ling L, Jin X (2012) A study of the derailment mechanism of a high speed train due to an earthquake. Vehicle System Dynamics 50:449–470.

Xu L, Zhai W (2017) Stochastic analysis model for vehicle-track coupled systems subject to earthquakes and track random irregularities. Journal of Sound and Vibration 407:209–225.

Yu J, Jiang L, Zhou W, et al (2020) Study on the dynamic response correction factor of a coupled high-speed train–track–bridge system under near-fault earthquakes. Mechanics Based Design of Structures and Machines 1–19.

Z., Y., SHEN, et al (1983) A Comparison of Alternative Creep Force Models for Rail Vehicle Dynamic Analysis. Vehicle System Dynamics

Zeng Q, Dimitrakopoulos EG (2018) Vehicle–bridge interaction analysis modeling derailment during earthquakes. Nonlinear Dyn 93:2315–2337.

Zeng Q, Guo X (1999) Theory and Application of Vibration Analysis of Train-Bridge Time-Dependent System. China railway Publishing House, Beijing

Zeng Z-P, Zhao Y-G, Xu W-T, et al (2015) Random vibration analysis of train–bridge under track irregularities and traveling seismic waves using train–slab track–bridge interaction model. Journal of Sound and Vibration 342:22–43.

Zhang Y, Jiang L, Zhou W, et al (2020) Study of bridge-subgrade longitudinal constraint range for high-speed railway simply-supported beam bridge with CRTSII ballastless track under earthquake excitation. Construction and Building Materials 241:118026.

Zhang ZC, Lin JH, Zhang YH, et al (2010) Non-stationary random vibration analysis for train–bridge systems subjected to horizontal earthquakes. Engineering Structures 32:3571–3582.

(2019) https://ngawest2.berkeley.edu